J. Cell. Mol. Med. Vol 14, No 8, 2010 pp. 2132-2143

Involvement of HAb18G/CD147 in T cell activation and immunological synapse formation

Jinsong Hu [a, #], Nana Dang [b, #], Hui Yao [a, #], Yu Li [a], Hongxin Zhang [a], Xiangmin Yang [a], Jing Xu [a], Huijie Bian [a], Jinliang Xing [a], Ping Zhu[c, *], Zhinan Chen [a, *]

[a] State Key Laboratory of Cancer Biology, Cell Engineering Research Centre & Department of Cell Biology, Fourth Military Medical University, Xi'an, People's Republic of China
[b] State Key Laboratory of Cancer Biology, Department of Biochemistry and Molecular Biology, Fourth Military Medical University, Xi'an, People's Republic of China
[c] Department of Clinical Immunology, Xijing Hospital, Fourth Military Medical University, Xi'an, People's Republic of China

Received: September 19, 2008; Accepted: April 24, 2009

Abstract

HAb18G/CD147, a glycoprotein of the immunoglobulin super-family (IgSF), is a T cell activation-associated molecule. In this report, we demonstrated that HAb18G/CD147 expression on both activated $CD4^+$ and $CD8^+$ T cells was up-regulated. *In vitro* cross-linking of T cells with an anti-HAb18G/CD147 monoclonal antibody (mAb) 5A12 inhibited T cells proliferation upon T cell receptor stimulation. Such co-stimulation inhibited T cell proliferation by down-regulating the expression of CD25 and interleukin-2 (IL-2), decreased production of IL-4 but not interferon-γ. Laser confocal imaging analysis indicated that HAb18G/CD147 was recruited to the immunological synapse (IS) during T cell activation; triggering HAb18G/CD147 on activated T cells by anti-HAb18G/CD147 mAb 5A12 strongly dispersed the formation of the IS. Further functional studies showed that the ligation of HAb18G/CD147 with mAb 5A12 decreased the tyrosine phosphorylation and intracellular calcium mobilization levels of T cells. Through docking antibody–antigen interactions, we demonstrated that the function of mAb 5A12 is tightly dependent on its specificity of binding to N-terminal domain I, which plays pivotal role in the oligomerization of HAb18G/CD147. Taken together, we provide evidence that HAb18G/CD147 could act as a co-stimulatory receptor to negatively regulate T cell activation and is functionally linked to the formation of the IS.

Keywords: HAb18G/CD147 • T cell activation • co-stimulatory molecule • lipid rafts • IS • molecular modelling and docking

Introduction

Proper T cell activation is central to the generation of protective adaptive immunity and in the maintenance of self-tolerance. T cell activation is initiated when the T cell receptor (TCR) encounters major histocompatibility complex (MHC)-specific antigen peptide complexes and co-stimulatory ligands on the surface of an antigen-presenting cell (APC). TCR stimulation delivers the primary signal necessary for the activation of resting T cells. Co-stimulation is crucial in determining antigen-specific T cell activation and tolerance and it provides both positive and negative signals that modulate the intensity, temporal extension and termination of the T cell response to a specific antigenic stimulation [1]. The best studied co-stimulatory ligands are B7–1 and B7–2, which are highly expressed by activated APC and function through their positive receptor CD28 on resting and activated T cells [2]. An inhibitory co-stimulatory receptor CTLA-4, induced after T cell activation, provides strong negative signals to maintain the appropriate threshold of T cell activation [3]. More recently, multiple other co-stimulatory receptor/ligand pairs that integrate into stimulatory or inhibitory activity for T cells have been identified, including inducible T cell co-stimulator (ICOS)/ B7-H2, PD-1/B7-H1, PD-L2/B7-DC, OX40/OX40L, 4–1BB/4–1BBL, CD40/CD154, CD27/CD70 (CD27L), T cell immunoglobulin and mucin protein-1 (Tim-1)/Tim-4 [4–11].

T cell activation is based on interactions of T cell antigen receptors with MHC-peptide complexes in a specialized cell–cell junction between the T cell and APC. The interactions can induce dramatic T cell polarization and the formation of a specialized

[#]These authors contributed equally to this study.
*Correspondence to: Zhinan CHEN, Ping ZHU,
Cell Engineering Research Centre & Department of Cell Biology,
Fourth Military Medical University, Xi'an 710032,
People's Republic of China.
Tel.: ++86(29)84774547
Fax: ++86(29)83226349
E-mail: znchen@fmmu.edu.cn, zhuping@fmmu.edu.cn

doi:10.1111/j.1582-4934.2010.01012.x

immunological synapse (IS) at the T cell–APC junction [12, 13]. Recent studies indicate that the organized immunological synapse is a multitasking platform performing several functions essential to the determination of TCR sensitivity and responsiveness. The IS enhances TCR engagement and signal transduction through the recruitment, concentration, and juxtaposition of receptors and transducers [12, 14].

CD147 is a 50–60 kD transmembrane glycoprotein that was categorized as a member of the immunoglobulin super-family (IgSF) [15, 16]. CD147 is also known throughout the literature as M6 antigen [17], basigin [18], extracellular matrix metalloproteinase inducer and HAb18G independently [16, 19, 20]. Previously functional studies revealed that CD147 is a pleiotropic molecule and plays a very important role in foetal, neuronal and lymphocyte development. In addition, it has been associated with pathological conditions such as heart disease, Alzheimer's disease, stroke, tumour, inflammation and autoimmune disease [21–30].

CD147 was identified as a lymphocyte development and activation-associated antigen [15, 17]. Within the thymus, CD147 expression is highest on late stage and correlates with cycling of immature thymocytes even in the absence of TCR-β selection. Treatment of immature foetal lymphocytes with an anti-CD147 monoclonal antibody arrested any further development, suggesting the importance of CD147 in T cell differentiation [31]. Within circulating immune cell populations, CD147 is expressed on the surface of all immune cells, but increased on activated T cells [32, 33]. Overexpressed CD147 was also found on $CD3^+$ T lymphocytes from systemic lupus erythematosus patients when compared with $CD3^+$ T lymphocytes from healthy donors [28]. As a potential cell surface receptor for cyclophilin A and cyclophilin B, CD147 is required for enhancing effect of cyclophilin on T cell adhesion and can enhance cyclophilin-mediated chemotatic activities during inflammatory responses [26, 34]. In addition, CD147 knockout mice are characterized by enhanced mixed lymphocyte responses, indicating a potential negative regulatory function of CD147 in T cell regulation [35]. However, to date, the exact role of CD147 in T cell activation remains unclear.

In this study, the molecular function of HAb18G/CD147 in regulating of T cell activation was investigated. To begin with, we found that the expression of HAb18G/CD147 was up-regulated on both activated $CD4^+$ and $CD8^+$ T cells. The further studies by confocal microscopy and Western blot revealed that the up-regulated HAb18G/CD147 was recruited to the IS. Then, we tested four HAb18G/CD147 mAbs generated in our laboratory and found the engagement of HAb18G/CD147 with mAb 5A12 strongly inhibited T cell proliferation and up-regulated the production of interferon (IFN)-γ, whereas down-regulated the secretion of both interleukin-2 (IL-2) and IL-4. Furthermore, confocal microscopy imaging analysis revealed that the HAb18G/CD147 mAb 5A12 disrupted the formation of the IS. Finally, examination of key signalling intermediates showed that TCR proximal events such as global tyrosine phosphorylation, intracellular Ca^{2+} elevation are also perturbed by engagement of HAb18G/CD147 with mAb 5A12. These data demonstrate the importance of HAb18G/CD147 in reorganization of IS and the negative co-stimulatory role of HAb18G/CD147 towards optimal T cell activation.

Materials and methods

Abs and reagents

The monoclonal antibodies (3B3, 5A12, 6H8, HAb18) against HAb18G/CD147 were generated and identified in our lab. Mouse anti-Japanese B Encephalitis mAb was a kind gift from the department of microbiology (Fourth Military Medical University, People's Republic of China), and used as isotype-matched irrelevant control (IgG1). Anti-CD3 mAb (clone HIT3a), anti-CD28 mAb (clone CD28.2) were purchased from BD Pharmingen (San Diego, CA, USA). FITC-conjugated mouse anti-human CD4, FITC-conjugated mouse anti-human CD8, APC-conjugated mouse anti-human CD3 were purchased from BioLegend (San Diego, CA, USA). RPE-conjugated mouse anti-human CD147 was obtained from AbD Serotec (Oxford, UK). FITC-conjugated mouse anti-human CD25 was purchased from eBioscience (San Diego, CA, USA). FITC-conjugated mouse anti-human CD48 and FITC-conjugated cholera toxin B subunit and staphylococcus enterotoxin B (SEB) were all from Sigma-Aldrich (St Louis, MO, USA). The antibodies (Abs) used for Western blot were as follows: anti-Rab5 (ab18211, Abcam, Cambridge, UK), anti-Fyn (ab24051, Abcam), anti-phosphotyrosine 4G10 (Millipore, Billerica, MA, USA). Cell Tracker Blue, CMAC (7-amino-4-chloromethylcoumarin) were purchased from Molecular Probes (Eugene, OR, USA).

Isolation and purification of T cells

Peripheral blood was obtained from healthy volunteers following informed consent. Briefly, peripheral blood mononuclear cells were isolated from heparinized venous blood density gradient centrifugation over Ficoll according to the manufacturer's instructions. T cells were subsequently purified from peripheral blood mononuclear cells by two passages over nylon wool columns, as described previously [36]. Single cell suspensions were applied to prerinsed nylon-wool columns. After incubation in an upright position at 37°C for 90 min., the non-adherent cells were eluted from the columns. Purity of the resulting population was checked by flow cytometry with APC-conjugated anti-CD3. Purified T cells were consistently 85–95% CD3 positive.

T cell proliferation assay

To determine the influence of the HAb18G/CD147 mAbs on T cell proliferation, purified T cells were cultured under the various conditions, as described in the figure legends. 96-well flat-bottom plates (Nunc, Roskilde, Denmark) were coated with anti-CD3 mAb (1 μg/ml) overnight. After washing precoated plates twice, triplicate aliquots of 1×10^5/well purified T cells in a final volume of 200 μl were cultured with immobilized anti-CD3 mAb in the presence or absence of anti-HAb18G/CD147 mAbs (10 μg/ml) and/or anti-CD28 mAb (10 μg/ml). The cultures were grown at 37°C and 5% CO_2 in a humidified atmosphere for 3 days, then 1 μCi of [^{3}H]-thymidine (Beijing Atom HighTech, Beijing, People's Republic of China) was added 18 hrs before harvesting. Incorporated radioactivity was measured by a liquid scintillation counter (Packard Instrument, Meriden, CT, USA).

Flow cytometry

Purified T cells were activated as described above (see T cell proliferation assay). Analysis of cell surface expression of CD147 and CD25 was

performed 24 hrs after culture initiation. T cell samples were treated with 0.5% goat serum for 15 min. at 4°C to block the Fc receptor. Aliquots of cells (5×10^5 cells) were stained with FITC-conjugated CD4 or CD8, PE-conjugated CD147 or FITC-conjugated CD25 for 30 min. at 4°C. After washing twice, membrane fluorescence was analysed on a FACS Calibur flow cytometer (Beckman Coulter, CA, USA). Ten thousand events were acquired from the viable cells gated based on forward scatter and side scatter and analysed for the expression of various marker proteins using relevant antibodies. The flow cytometry data were analysed using WinMDI software written by Joe Trotter (The Salk Institute, Flow Cytometry Laboratory, La Jolla, CA, USA).

Cytokine ELISA

For cytokine measurement culture supernatants under different conditions were harvested after 72 hrs and cytokines IFN-γ, IL-2 and IL-4 levels were measured by ELISA according to the manufacturer's instructions (R&D Systems, Minneapolis, MN, USA).

Capping and immunofluorescence microscopy

All procedures were performed at 0–4°C unless otherwise described. Purified resting T cells were suspended at 1×10^6 cells/ml and incubated with anti-CD3 (1 μg/ml) and anti-CD28 (10 μg/ml) for 2 hrs at 37°C. After capping, cells were washed with ice-cold Hanks'/0.1% sodium azide and then fixed immediately in 1 ml 4% formaldehyde–Hanks balanced salt solution, stained with FITC-conjuated anti-CD4 (or CD8), FITC-conjuated anti-CD48, PE-conjuated anti-CD147. After washing with ice-cold Hanks'/0.1% sodium azide again, cells were then plated onto glass cover slips, mounted in glycerol/phosphate-buffered solution (PBS), and examined by an Olympus confocal microscope (Olympus FluoView1000, Tokyo, Japan). Appropriate excitation and barrier filters were used to observe fluorescence. Photographs of cells shown in figures represent the majority of cells displaying cell-surface staining pattern. For evaluation of colocalization, cells were visualized by Olympus confocal laser scanning microscope and analysed with an Olympus FluoView Software FV10-ASW (version 1.6) and ImageJ (http://rsb.info.nih.gov/ij/index.html). The percentage of cells showing cap was assessed by analysing the distribution of the fluorescence intensity on the cell membrane. Cells displaying a 3-fold increase of fluorescence intensity on one site of the cell membrane were counted as cells with caps. Two hundred cells per sample were analysed. For image presentation, size and contrast were adjusted with Photoshop 7.0 software (Adobe Software, Palo Alto, CA, USA).

For cholera toxin colocalization, T cells were treated with FITC-labelled cholera toxin B subunit on ice for 30 min., followed by treatment with goat anti-cholera toxin B subunit on ice for 30 min. Cells were then placed at 37°C for 10 min. to allow cross-linking, adhered to cover slips, fixed, stained, and analysed by immunofluorescent microscopy as above.

Conjugate formation and analysis

For B and T cell conjugations, Raji B-lymphocytes were loaded with 10 μM CMAC for 30 min. at 37°C, washed, and resuspended in RPMI 1640 with 10% FBS. Cells were then incubated for 15 min. in the absence or presence of 1 μg/ml SEB. Jurkat cells were mixed with an equal number of Raji cells in a final volume of 50 μl and were incubated at 37°C for 15 min. Conjugates were plated on poly-D-lysine–coated slides, fixed for 10 min. in 4% formaldehyde–Hanks balanced salt solution and were stained with the appropriate antibodies. Cells were visualized with an Olympus confocal laser scanning microscope (Olympus FluoView1000). Images were acquired and analysed and adjusted as described before.

Isolation of the lipid rafts

T cells were stimulated as described above, 2×10^8 T cells were pelleted, and lysed with 1 ml of ice-cold MBS lysis buffer (0.5% Triton X-100, 50 mM Tris [pH 7.6], 150 mM NaCl, 5 mM ethylenediaminetetraacetic acid, 1 mM Na3VO4, 10 μg/ml aprotinin, 10 μg/ml leupeptin and 1 mM PMSF) on ice. Following 30 min. incubation on ice, the lysates were homogenized with 20 strokes of a loose-fitting Dounce homogenizer, gently mixed with an equal volume of 80% sucrose (w/v) in TNE buffer (20 mM Tris [pH 8.0], 150 mM NaCl, 50 mM ethylenediaminetetraacetic acid). The samples were then placed in the bottom of a SW40Ti centrifuge tube and overlaid with 2 ml of 30% sucrose (w/v) and 1 ml of 5% sucrose (w/v) in TNE buffer and centrifuged at 80,000 rpm using a Beckman Type 100 Ti rotor (Beckman Coulter, Fullerton, CA, USA) at 4°C for 3 hrs. After centrifugation, 9×0.55 ml fractions (excluding the pellet) were harvested serially from the top of the gradient. Fractions 1–4 (raft fractions) or fractions 7–9 (cytosol/heavy membrane nonraft fractions) were pooled, and aliquots were separated by SDS-PAGE. Sucrose fractions were then analysed by Western blot with HAb18, anti-Fyn and anti-Rab5 antibodies. Western blot analysis was performed according to standard protocol, the optical density of band was quantified by program ImageJ.

Analysis of protein tyrosine phosphorylation

Purified human T cells (5×10^6/condition) were stimulated with immobilized anti-CD3 mAb (1 μg/ml) in the presence of 10 μg/ml of anti-CD28 mAb and/or anti-CD147 mAb or isotype-matched irrelevant control mAb followed by cross-linking with antimouse IgG (1:200) for 2 hrs at 37°C in a CO_2 incubator. After washing, cells were immediately lysed in lysis buffer (PBS pH7.0 containing 1% NP-40, 5 mM idoacetamide, 5 mM aprotinin, and 1 mM PMSF) for 30 min. at 4°C. After centrifugation, soluble cell lysate samples were separated by 10% SDS-PAGE and Western blot with anti-phosphotyrosine Ab 4G10.

Calcium flux analysis

Purified T cells were suspended at 1×10^7/ml in 2% FBS/PBS containing 5 μM Fluo-3/AM (DOJINDO, Kumamoto, Japan) and incubated at 37°C for 30 min. Fluo-3-loaded cells were washed twice and resuspended at 5×10^6/ml in PBS. Then, cells were incubated in a water bath at 37°C for 5 min., followed by FACS Calibur flow cytometer. To establish a baseline, cells were acquired for 30 sec., at which point antibodies were added, and acquisition of cells was continued for 10 min. The calcium response was initiated by 1 μg/ml anti-CD3 or 1 μg/ml anti-CD3 plus 10 μg/ml anti-CD28 in combination with 10 μg/ml 5A12 or isotype-matched irrelevant control mAb.

Molecular modelling and docking of anti-HAb18G/CD147 mAbs to extracellular portion of HAb18G/CD147

The method of modelling and docking has been described previously [36]. Briefly, the light chain variable region and heavy chain variable region genes of anti-HAb18G/CD147 mAbs were cloned and sequenced. Molecular modelling and automated docking of monoclonal antibody and antigen were performed with MODELLER9V1 and AUTODOCK3.0, respectively. All the molecular models were refined with the DISCOVER module of INSIGHTII2000 (Molecular Simulations Inc., San Diego, CA, USA).

Statistical analysis

All data are representative of at least three different experiments. Values are expressed as mean ± S.D. Significant differences between two experimental groups were analysed by Student's t-test. Wherever stated, ns denotes a *P*-value of >0.05, while * indicates a *P*-value <0.05, ** indicates a *P*-value <0.01, and *** indicates a *P*-value <0.001. *P*-value of less than 0.05 was considered as significant.

Results

Expression of HAb18G/CD147 on T lymphocytes

We examined the cell surface expression pattern of HAb18G/CD147 on resting T cells and activated T cells by flow cytometry. HAb18G/CD147 expression was detectable on both resting $CD4^+$ and $CD8^+$ T cells and significantly increased on both $CD4^+$ (Fig. 1A) and $CD8^+$ (Fig. 1B) T cells after 24 hrs upon anti-CD3 and anti-CD28 mAb stimulation. The results strongly suggest that the expression of HAb18G/CD147 on subsets of $CD4^+$ and $CD8^+$ T cells is correlated with activation state.

Specific recruitment of HAb18G/CD147 to the IS

Many immune cell signalling reactions are mediated by lipid rafts-associated membrane proteins. In T cells, a prerequisite for efficient induction of membrane proximal signalling events *via* TCR is the formation of the IS at the site of TCR engagement [37, 38]. Membrane compartmentation and raft integrity triggered by TCR stimulation reorganize the distribution of signalling molecules. Many signalling proteins are enriched into IS during T cell activation. Therefore, we studied whether HAb18G/CD147 appears at the cap of activated T cell or at the interface between T cell and APC. For this purpose, the distribution of HAb18G/CD147, CD4, CD8, lipid rafts maker CD48 and ganglioside M1 (GM1) in resting and activated T cells was visualized by laser confocal microscopy. First, we analysed whether these molecules distribute into the T cell cap induced by CD3/CD28 co-stimulation. As can be seen in Fig. 2A–D, HAb18G/CD147, CD4/CD8, CD48 and GM1 were diffusely localized on the cell membrane in the non-stimulated state and co-capped after T cell activation. To further confirm this, we isolated the lipid rafts and detected the localization of HAb18G/CD147. As shown in Fig. 2E, Western blot analysis validated that HAb18G/CD147 was markedly accumulated in the raft fraction upon T cell activation. Furthermore, we verified whether HAb18G/CD147 translocates to the IS at T-B cell contact sites. In this study we labelled Raji B lymphocytes with CellTracker Blue CMAC and then incubated with Jurkat T cells in the absence or presence of SEB. In the absence of SEB, no enrichment of HAb18G/CD147, GM1 and CD48 occurred at the sites of contact between the Raji B lymphocytes and Jurkat T cells. In contrast, marked HAb18G/CD147, GM1, and CD48 recruitment appeared at the T-B cell interface in the presence of SEB (Fig. 3). Taken together, these observations show that HAb18G/CD147 is recruited to the IS or co-caps with lipid rafts markers and suggest the requirement of HAb18G/CD147 for T cell activation.

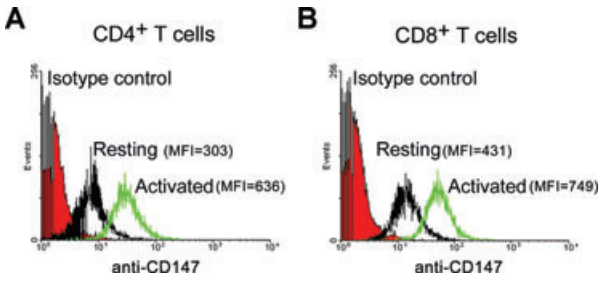

Fig. 1 Measurement of HAb18G/CD147 expression on resting and activated $CD4^+$ and $CD8^+$ T cell subsets. Purified resting T cells and activated T cells were stained with PE- conjugated anti-CD147, FITC-conjugated anti-CD4 or CD8, and were analysed by flow cytometry. (**A**) Histogram shows expression of CD147 on resting and activated $CD4^+$ T cells. (**B**) Histogram shows expression of CD147 on resting and activated $CD8^+$ T cells. These data are representative of a minimum of three separate experiments.

Ligation of HAb18G/CD147 with mAb 5A12 strongly inhibits T cell proliferation

Four HAb18G/CD147 mAbs, designated 3B3, 5A12, 6H8, and HAb18 were established in our laboratory [39]. In this study, T cells purified from healthy donors were stimulated with immobilized anti-CD3 mAb (plus soluble anti-CD28) in the presence or absence of various kinds of HAb18G/CD147 mAbs. As shown in Fig. 4, mAb 5A12 strongly inhibited the T cell proliferative response upon anti-CD3 (plus anti-CD28) stimulation, whereas all other HAb18G/CD147 mAbs (3B3, 6H8 and HAb18) and isotype-matched irrelevant control mAb did not affect T cell proliferation. In addition, 5A12, 3B3, 6H8 and HAb18 alone failed to affect T cell proliferation. Moreover, cell cycle analysis shows that mAb 5A12 can arrest cell cycle in G1 phase (see Fig. S1). These data

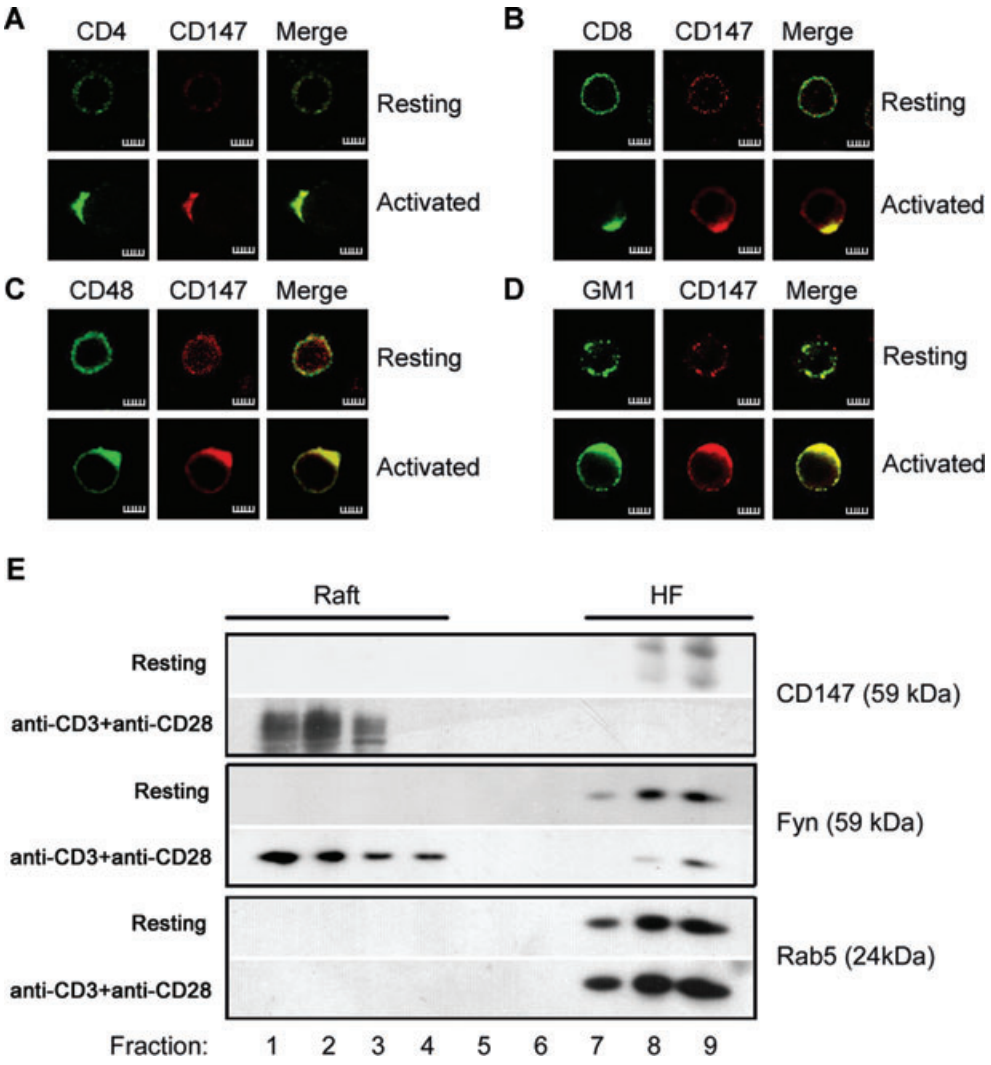

Fig. 2 HAb18G/CD147 accumulates to the cap and lipid rafts in T cells upon TCR stimulation confirmed by confocal microscopy and Western blot. (**A**, **B**, **C**, **D**) HAb18G/CD147 co-caps with CD4/CD8/CD48/GM1. T cells were prepared and stained as described previously in 'Materials and methods'. HAb18G/CD147, TCR co-receptor CD4 and CD8, lipid raft marker CD48 and GM1 diffusely distribute on the cell membrane of resting T cells (upper panel of Fig. 2A–D), whereas stimulation results in translocation of these molecules to the cap induced by TCR/CD3 (lower panel of Fig. 2A–D), scale bar, 5 μm. (**E**) HAb18G/CD147 is recruited to lipid rafts upon T cell activation. Lipid rafts were isolated as described previously in 'Materials and methods'. Sucrose fractions were analysed by Western blot with HAb18, anti-Fyn and anti-Rab5 antibodies. Detergent-insoluble membrane fractions containing isolated rafts were identified by the presence of the raft marker protein Fyn. Non-raft components of the membrane (*e.g.* Rab5) were purified in the heavy fraction (HF). HAb18G/CD147 appeared constitutively in the HF (7–9) with the non-raft marker Rab5 in resting T cells, a significant fraction of HAb18G/CD147 was localized within raft fractions (1–4) after T cell activation.

collectively indicate that ligation of HAb18G/CD147 might provide a negative signal for T cell proliferation.

Effects of HAb18G/CD47 mAb 5A12 on CD25 expression and cytokine secretion

CD25 is a well characterized marker for T cell activation. We evaluated the effect of the HAb18G/CD147 mAb 5A12 on CD25 expression on T cell in response to various activation stimuli. Quantitative flow cytometry confirmed that CD25 density on activated T cell population was down-regulated by the ligation of HAb18G/CD147 with mAb 5A12 (Fig. 5A). We further analysed whether mAb 5A12 affects the secretion of IL-2, IL-4 and IFN-γ. As shown in Fig. 5B–D, the production of IFN-γ from T cell culture supernatants was significantly up-regulated by the ligation of HAb18G/CD147 with mAb 5A12 upon TCR/CD3 stimulation and CD3/CD28 co-stimulation in comparison to that of other

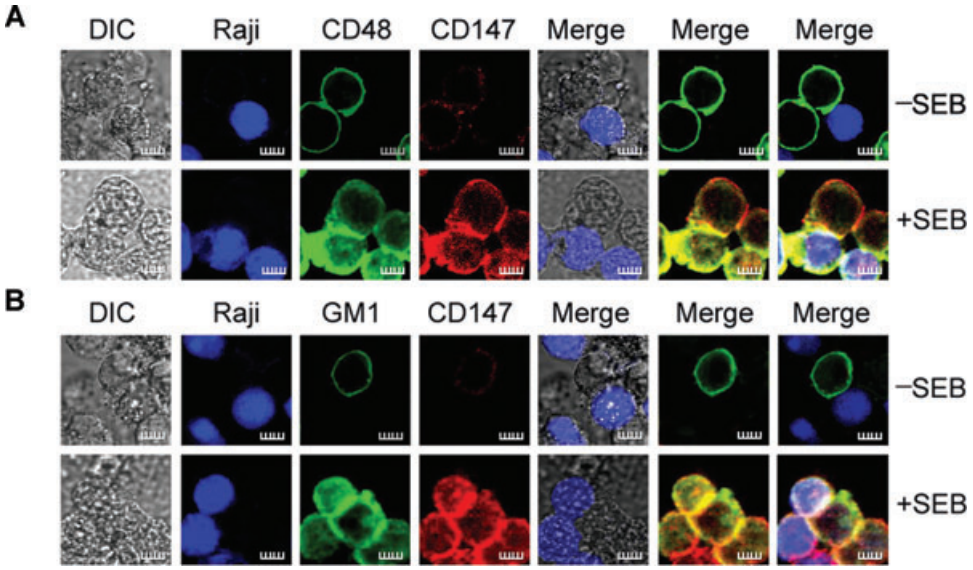

Fig. 3 HAb18G/CD147 together with CD48 and GM1 are enriched into the IS. Raji cells were labelled with the blue fluorescent cytoplasmic probe CMAC first. Jurkat cells were then incubated with CMAC-labelled and 1 μg/ml of SEB-loaded (or not) Raji cells. Conjugates were then plated onto cover slip, fixed, stained with antibodies to HAb18G/CD147 and to CD48 (Fig. 3A) or GM1 (Fig. 3B), and visualized by confocal fluorescence microscopy. The red and green images represent the localization and distribution of HAb18G/CD147 and CD48/GM1, respectively. Raji cells are shown in blue. Scale bar, 5 μm.

HAb18G/CD147 mAbs and isotype-matched control mAb, whereas the levels of IL-2 and IL-4 were decreased. These findings suggest that the influence of cross-linking HAb18G/CD47 with mAb 5A12 on T cell activation is related to the changes of cytokine secretion pattern, indicating that HAb18G/CD147 may play a unique role in T cell immune response.

Ligation HAb18G/CD147 with mAb 5A12 interferes with formation of the IS

Disturbance of the structural integrity of IS inhibits T cell activation [40, 41]. Therefore, we evaluated the possibility that HAb18G/CD147 mAb 5A12 inhibition of T cell proliferation is associated with reorganizing lipid rafts. As can be seen from Fig. 6, resting T cells showed a diffuse or ring pattern cell membrane staining, whereas approximately 80% activated T cells showed accumulation of lipid rafts marker CD48 to a polarized surface cap. When T cells were stimulated with anti-CD3 mAb in the presence of mAb 5A12, the percentage of cells showing cap reduced to approximately 15%, in comparison with the approximately 80% value in the cells treated with isotype-matched irrelevant control mAb or other non-functional HAb18G/CD147 mAbs (3B3, 6H8, HAb18, data not shown). These results indicate that HAb18G/CD147 mAb 5A12 can disorganize the accumulation of lipid rafts upon T cell activation.

HAb18G/CD147 mAb 5A12 decreases intracellular calcium mobilization

The precise control of T cell activation relies on cytosolic Ca^{2+} dynamics that is shaped by the Ca^{2+} release from the intracellular

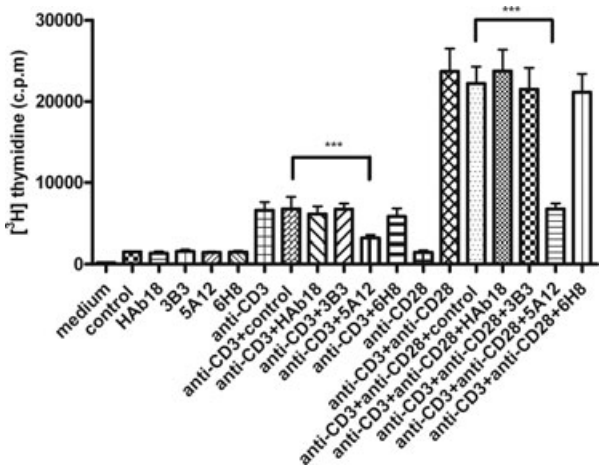

Fig. 4 Influence of HAb18G/CD147 mAbs on T cell proliferation. Proliferation was determined on day 4 following stimulation as described in 'Materials and methods'. This figure shows the [^{3}H]-thymidine incorporation in c.p.m. (mean ± S.D. of triplicated wells). Data are a representative of three independent experiments. ***, $P < 0.001$.

store and extracellular Ca^{2+} influx. The Ca^{2+} influx activation following TCR-mediated store depletion is considered to be a major mechanism for the sustained elevation in cytosolic Ca^{2+} concentration ([Ca^{2+}]i) necessary for T cell activation. It is established that TCR stimulation leads to production of numerous second messengers, including 1,4,5-trisphosphate (IP3), which evokes Ca^{2+} release from the 1,4,5-trisphosphate receptor (IP3R), located predominantly on the endoplasmic reticulum [42]. To further investigate the possible signalling pathway involved in the inhibitory role of HAb18G/CD147 in T cell activation, we measured

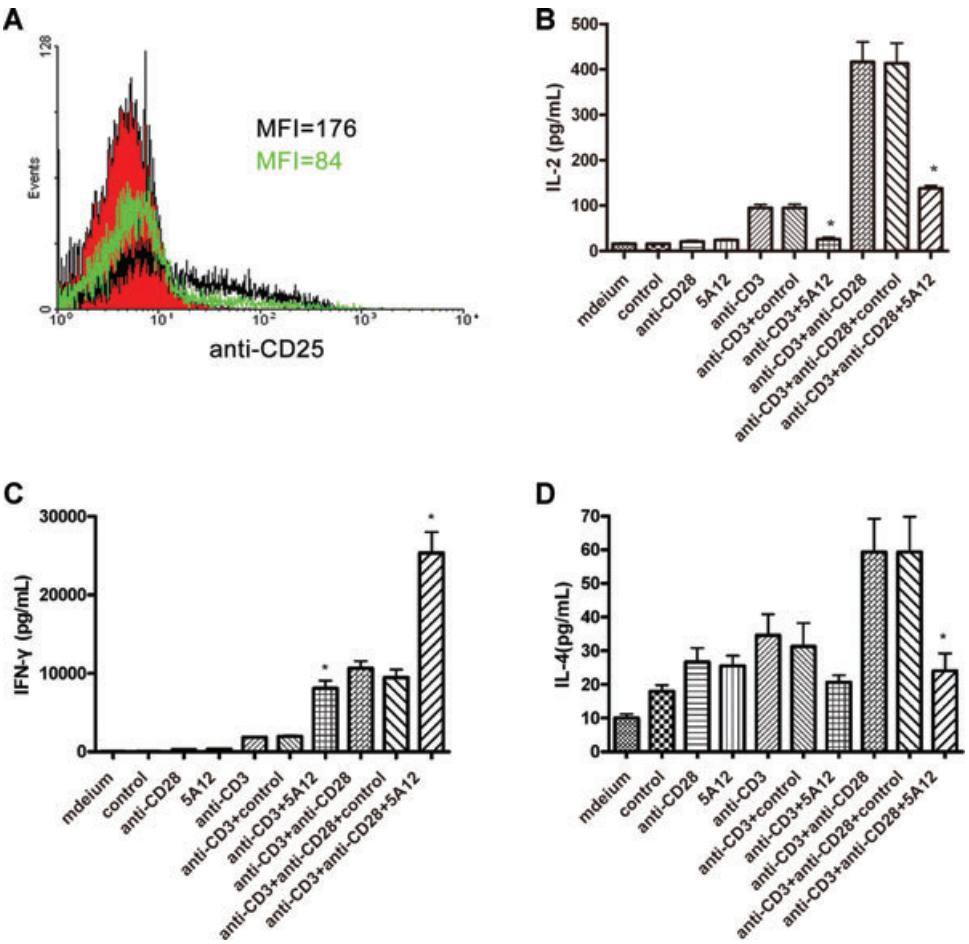

Fig. 5 Cross-linking of HAb18G/CD147 with mAb 5A12 affects surface expression of CD25 and cytokine production. (**A**) mAb 5A12 down-regulates surface expression of CD25. Red-tinted histogram represents isotype control. Black and green lines represent anti-CD3 mAb plus isotype-matched irrelevant control mAb (mouse IgG1) or 5A12 intervention, respectively. (**B**, **C**, **D**) mAb 5A12 decreases IL-2 and IL-4 but increases IFN-γ production. Purified T cells were stimulated with immobilized 1 μg/ml of anti-CD3 mAb or 1 μg/ml of anti-CD3 mAb plus 10 μg/ml anti-CD28 mAb in the presence of 10 μg/ml mAb 5A12 or isotype-matched irrelevant control for 72 hrs. Bar graphs, (mean ± S.D.) levels of IL-2, IL-4 and IFN-γ in culture supernatants as measured by ELISA. *, $P < 0.05$.

the cytosolic Ca^{2+} concentration upon TCR stimulation in the presence of HAb18G/CD147 mAb 5A12 by flow cytometry. As shown in Fig. 7A, stimulation of resting T cells started when CD3 mAb plus isotype-matched control mAb were added (indicated by an arrow in the figure) and resulted in an increase of $[Ca^{2+}]_i$, followed by a lesser extent response. $[Ca^{2+}]_i$ was increased upon CD3 engagement but was reduced by CD147/5A12 engagement. Stimulation of CD3/CD28 plus mAb 5A12 also induced a lower $[Ca^{2+}]_i$ increase when compared to CD3/CD28 plus isotype-matched control mAb. Cross-linking of HAb18G/CD147 by mAb 5A12 alone did not induce any response.

HAb18G/CD147 affects protein tyrosine phosphorylation upon CD3/TCR stimulation

To further explore the role of HAb18G/CD147 in the T cell activation signalling pathway, the influence of mAb 5A12 on CD3-induced tyrosine phosphorylation was examined (Fig. 7B). CD3/CD28 co-stimulation resulted in a strong tyrosine phosphorylation of proteins in the zone of 45 to 130 kD band(s). Phosphorylation of the band(s) around the zone of 45 to 130 kD induced by CD3/CD28 ligation was partly inhibited in the presence of mAb 5A12 in comparison to isotype-matched control mAb. The presence of mAb 5A12 also partially inhibited CD3-induced tyrosine phosphorylation in comparison to isotype-matched control mAb. The ligation of HAb18G/CD147 with mAb 5A12 alone did not induce significant changes in protein tyrosine phosphorylation.

mAb 5A12 is specifically docked to N-terminal domain I of HAb18G/CD147

The sequences of the heavy chain Fd fragment and light chain of HAb18, 5A12 and 6H8 were cloned and analysed (Fig. S2). We found that the variable regions (Fv) of the three anti-HAb18G/CD147 mAbs are different. By using computer-assisted molecular modelling and docking, the interactions of HAb18G/CD147 epitope antigen with specific anti-HAb18G/CD147 mAbs were examined. It was found that these three mAbs, HAb18,

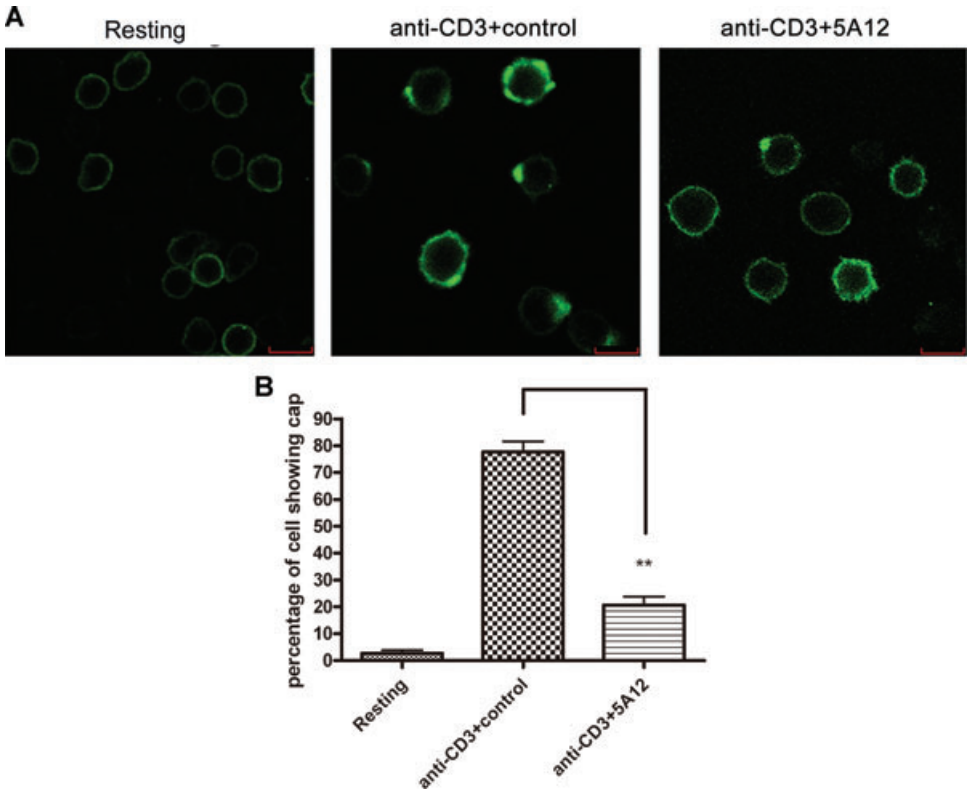

Fig. 6 Inhibition of anti-CD3 stimulated redistribution of the CD48 molecule by HAb18G/CD147 mAb 5A12. Purified peripheral blood T cells were cultured and stimulated with immobilized CD3 mAb in the presence or absence of 10 μg/ml of HAb18G/CD147 mAb 5A12 or isotype-matched irrelevant control mAb for 2 hrs. Then, cells were collected, fixed and stained with FITC-labelled CD48 as described in 'Materials and methods'. The percentage of cells showing cap was assessed by analysing the distribution of the fluorescence intensity on the cell membrane of CD48-FITC stained cells using FV10-ASW (version 1.6) software. The images are a representative of three experiments. Scale bar, 5 μm. **, $P < 0.01$.

5A12 and 6H8 have different conformations, and recognize different regions of HAb18G/CD147 (Fig. 8). Among these three mAbs, HAb18 binds with N-terminal of HAb18G/CD147 in the manner of head to head, 5A12 and 6H8 were typically docked to the N-terminal IgC2 domain I (amino acid residues 22–101) and C-terminal IgI domain I (amino acid residues 107–205), respectively. At the docked conformation, a number of amino acid residues of HAb18G/CD147 critical to the interactions were identified and listed as follows: (1) HAb18: Glu39, Thr51, Asp65; (2) 6H8: Ser145, Arg184, Asp194 and (3) 5A12: Thr25, Asp32, Glu84, Thr96, Gln100.

Discussion

Within the paradigm of the two-signal model of T cell activation, the interest in co-stimulation has witnessed a remarkable emergence in the past few years with the discovery of a large array of molecules that can serve this role, including some with inhibitory function. Furthermore, structure/function experiments and complementary pharmacological studies have also shown that cholesterol- and sphingolipid-enriched plasma membrane microdomains, also termed lipid rafts, control the localization and function of proteins which are components of signal pathways regulated TCR [43, 44]. Triggering TCR results in T cell reorganization of the related plasma membrane signal molecules in a concerted fashion, leads to the formation of a well-structured lipid rafts known as IS between the T cell and the APC during the initial period of activation. Immunological synapse is proposed to function as platform for signal transduction and cytoskeletal reorganization, as a consequence, perturbation of the structural integrity of IS inhibits TCR-induced T cell activation [40, 44].

The current study was to investigate the possible role of HAb18G/CD147 in T cell activation. We observed that HAb18G/CD147 expression was increased on both $CD4^+$ and $CD8^+$ T cells after activation. Given that the functional outcome of CD147 overexpression on activated T cells was not clearly assessed, it is necessary to account for its potential role in T cell biology. The following data further proved that up-regulated HAb18G/CD147 was translocated to the lipid raft compartment within the IS upon T cell activation. Significantly, TCR co-receptor CD4/CD8, lipid rafts marker CD48 and GM1 were also accumulated at the same site simultaneously. To our knowledge, this study first demonstrated the accumulation feature of HAb18G/CD147 within the IS upon T cell activation. The results might suggest an important role for HAb18G/CD147 in coordinating with CD4/CD8 and CD48 in synaptic lipid raft clustering and T cell activation. Furthermore, we investigated the influence of cross-linking of HAb18G/CD147 with antibody on the formation of the IS. We found that ligation of HAb18G/CD147 with mAb 5A12

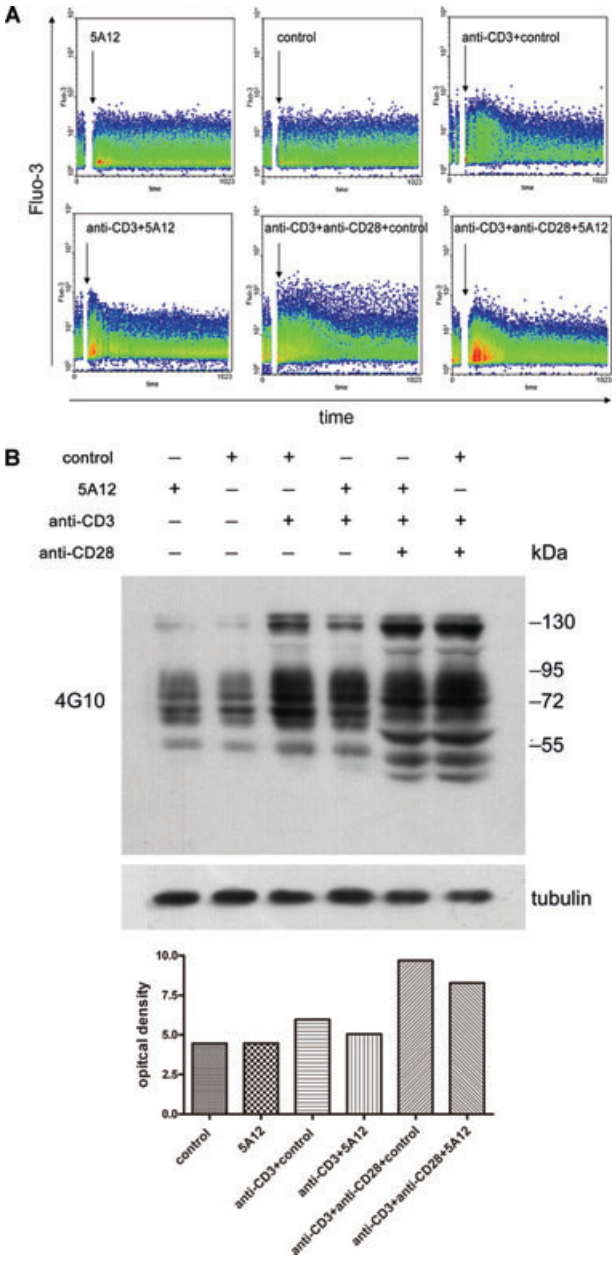

Fig. 7 Cross-linking of HAb18G/CD147 with mAb 5A12 affects intracellular signalling pathway upon T cell activation. (**A**) Extracellular Ca^{2+} influx triggered by TCR stimulation is inhibited by mAb 5A12. The figure is a representative of three experiments. (**B**) HAb18G/CD147 mAb 5A12 slightly decreases the tyrosine phosphorylation level upon TCR triggering. Purified T cells were stimulated using CD3 mAb (plus mAb CD28) in the presence of mAb 5A12 or isotype-matched irrelevant control. After 2 hrs of stimulation, the cells were lysed and analysed for tyrosine phosphorylation level using Western blot. The figure is a representative of three experiments. Top, the representative image; bottom, quantitative analysis of the image.

remarkably interfered with the formation of the IS, disturbed the accumulation of CD48 at the cap. This is in agreement with previous finding that the cross-linking of CD147 with antibodies can displace of CD48 from the lipid rafts [45]. These results indicate that HAb18G/CD147 contributions to synapse assembly might be more relevant to polarized delivery of effector molecules and down-regulation of TCR signals. Further elucidation of molecular mechanisms by which HAb18G/CD147 impacts TCR signal transduction and synapse formation should aid in understanding the pivotal role of HAb18G/CD147 playing in coordinating TCR engagement with functional outcome.

In most studies, the co-stimulation role of the ancillary surface molecule has been evaluated as the capacity of each mAb against these molecules to enhance or inhibit the proliferation of resting T cells stimulated with suboptimal doses of anti-CD3 [46]. Previous studies have shown that anti-CD147 mAb, MEM-M6/6 inhibited OKT3 induced T cell proliferation [28, 32]. In the present study we used a panel of newly established HAb18G/CD147 mAb in our lab to further characterize the molecule HAb18G/CD147, and found that only mAb 5A12 can inhibit CD3-TCR stimulated T cell proliferation through mimicking ligand engagement, in contrast to other anti-HAb18G/CD147 mAbs and isotype-matched irrelevant control mAb. T cell proliferation is growth factor dependent, one such T cell growth factor is IL-2 [47, 48]. Resting T cells express the intermediate affinity IL-2R$\beta\gamma$, but not the high affinity receptor component IL-2Rα (CD25). Upon stimulation of TCR, T cells express both CD25 and IL-2 [49]. To further elucidate the effects of engagement of HAb18G/CD147 on T cell activation, we investigated the secretion of IL-2 and expression of CD25. In this analysis, cross-linking of HAb18G/CD147 with mAb 5A12 impaired the secretion of IL-2 and expression of CD25. Moreover, cell cycle analysis also revealed a deceleration of G1->S/G2/M phase cell cycle progression induced by mAb 5A12. Thus, these findings, suggest strongly that HAb18G/CD147 could act as a negative regulatory receptor for T cell activation.

Th1/Th2 and Tc1/Tc2 cytokines also play regulatory roles in T cell activation. We found here that T cell expansion efficiency is associated with Th1/Th2 and Tc1/Tc2-related cytokine production. Cross-linking HAb18G/CD147 with mAb 5A12 resulted in significantly higher production of Th1/Tc1 cytokine IFN-γ, but decreased the secretion of Th2/Tc2 cytokine IL-4. IFN-γ is secreted by activated T cells and considered to be a Th1/Tc1 cytokine with immunomodulatory effects. The prevailing dogma of IFN-γ is that it drives T cell differentiation towards the Th1/Tc1 phenotype and suppresses Th2/Tc2 development. However, several new proofs indicate that high IFN-γ production is tightly associated with the inhibition of T cell proliferation. For example, the mechanism by which B7-H1 and B7-DC inhibit T cell proliferation is related to the enhanced IFN-γ production, because the inhibition of T cell proliferation by anti-B7-H1 mAb was abolished by neutralizing anti-IFN-γ mAb [50]. Experiments conducted in IFN-γ knockout mice further demonstrated that IFN-γ treatment can suppress T cell activation [51]. Taken together, markedly higher production of IFN-γ induced by ligation of

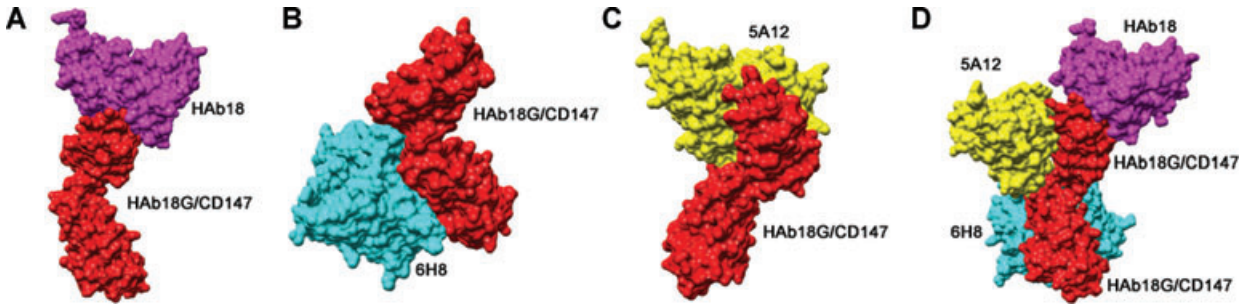

Fig. 8 Computer-assisted molecular docking of HAb18G/CD147 antigen-antibody complex. (**A**) The modelled structure of the variable domain of mAb HAb18 was docked to the most membrane-distal region of HAb18G/CD147 in a head-to-head manner. (**B**) The variable domain of mAb 6H8 was docked to C-terminal domain II of HAb18G/CD147. (**C**) The interaction between mAb 5A12 and HAb18G/CD147. The binding zone localizes at the functional N-terminal domain I. (**D**) Overview of docking the three mAbs to HAb18G/CD147 extracellular portion.

HAb18G/CD147 with mAb 5A12 in this study appears to be one of down-regulators of T cell activation.

The most immediate consequence of TCR activation is the initiation of signalling pathways including induction of specific protein tyrosine kinases, breakdown of phosphatidylinositol 4,5-biphosphate, activation of protein kinase C and elevation of intracellular Ca^{2+} concentration. As the results shown, cross-linking HAb18G/CD147 with mAb 5A12 slightly decreased tyrosine phosphorylation level upon TCR stimulation. Moreover, downstream Ca^{2+} released from the intracellular store and extracellular Ca^{2+} influx triggered by TCR stimulation was also inhibited by mAb 5A12. These findings show that certain signals can be transmitted *via* CD3 as well as CD28 in the presence of HAb18G/CD147 mAb 5A12 and indicate that HAb18G/CD147 might be an important safeguard that keeps T cell activation under the control of the TCR.

Structure studies on interacting antibody and antigen are highly beneficial to understanding of principles that govern the interaction. In this study, we found that mAb HAb18, 5A12 and 6H8 recognize different regions of HAb18G/CD147. In comparison with the C-terminal domain II binding feature of 6H8, the epitopes of HAb18, 3B3 and 5A12 localize at the N-terminal domain I. The docking studies further revealed that the epitopes recognized by mAb HAb18 and 3B3 localize at the regions adjacent to N-terminal of HAb18G/CD147, and are conformational independent [52, 53]. On the contrary, the epitope recognized by mAb 5A12 covers the major part of N-terminal domain I of HAb18G/CD147 and is conformational. In addition, we have previously demonstrated the existence of four kinds of dimerization manners by resolving the X-ray crystal structure of the soluble extracellular portion of HAb18G/CD147, which provides a good structural explanation for the multiple oligomerization-dependent functions of CD147 [52]. Considering that only N-terminal domain I of CD147 is functionally essential to oligomer formation, it is reasonable to conclude that the function of mAb 5A12 on T cell activation is tightly related to its specific binding characteristic with N-terminal domain I [54].

In conclusion, our current results demonstrated that combination of anti-HAb18G/CD147 with an activating mix of monoclonal antibodies to CD3 and CD3 plus CD28 targeting the TCR complex and the main co-stimulatory pathway profoundly inhibits T cell activation. Our data collectively show that HAb18G/CD147 could serve as a negative co-stimulatory receptor to regulate TCR-mediated response, the mechanism for down-regulation TCR activation tightly depends on the oligomerization of HAb18G/CD147 mediated by functional N-terminal domain I, and subsequent reorganization of the IS.

Acknowledgements

This work was supported by grants from the Ministry of Science and Technology of China (2006CB708500, 2009CB521704), the National Natural Science Foundation of China (30530720, 30700730) and the Natural Science Foundation of Shaanxi Province (2004C214).

Supporting Information

Additional Supporting Information may be found in the online version of this article:

Fig. S1 G1 phase cell cycle arrest provoked in T cells by mAb 5A12. Cell cycle distribution was assessed by flow cytometry analysis of propidium iodide-stained nuclei. The data were representative of three independently performed experiments.

Fig. S2 Molecular modelling of anti-HAb18G/CD147 mAbs. (**A**) Cloning and sequencing the heavy chain Fd and full-length light chain genes of mAb HAb18, 5A12, 6H8. Shadowed sequences indicate the PCR primers. (**B**) The modelled 3D structure of anti-HAb18G/CD147 mAb HAb18, 5A12 and 6H8.

Please note: Wiley-Blackwell are not responsible for the content or functionality of any supporting materials supplied by the authors. Any queries (other than missing material) should be directed to the corresponding author for the article.

References

1. **Janeway CA Jr, Medzhitov R.** Innate immune recognition. *Annu Rev Immunol.* 2002; 20: 197–16.
2. **Lenschow DJ, Walunas TL, Bluestone JA.** CD28/B7 system of T cell costimulation. *Annu Rev Immunol.* 1996; 14: 233–58.
3. **Chambers CA, Allison JP.** Costimulatory regulation of T cell function. *Curr Opin Cell Biol.* 1999; 11: 203–10.
4. **Hutloff A, Dittrich AM, Beier KC, *et al.*** ICOS is an inducible T-cell co-stimulator structurally and functionally related to CD28. *Nature.* 1999; 397: 263–6.
5. **Yoshinaga SK, Whoriskey JS, Khare SD, *et al.*** T-cell co-stimulation through B7RP-1 and ICOS. *Nature.* 1999; 402: 827–32.
6. **Sharpe AH, Freeman GJ.** The B7-CD28 superfamily. *Nat Rev Immunol.* 2002; 2: 116–26.
7. **Sugamura K, Ishii N, Weinberg AD.** Therapeutic targeting of the effector T-cell co-stimulatory molecule OX40. *Nat Rev Immunol.* 2004; 4: 420–31.
8. **Myers L, Lee SW, Rossi RJ, *et al.*** Combined CD137 (4–1BB) and adjuvant therapy generates a developing pool of peptide-specific CD8 memory T cells. *Int Immunol.* 2006; 18: 325–33.
9. **Yasumi T, Katamura K, Yoshioka T, *et al.*** Differential requirement for the CD40-CD154 costimulatory pathway during Th cell priming by CD8 alpha+ and CD8 alpha- murine dendritic cell subsets. *J Immunol.* 2004; 172: 4826–33.
10. **Arens R, Tesselaar K, Baars PA, *et al.*** Constitutive CD27/CD70 interaction induces expansion of effector-type T cells and results in IFNgamma-mediated B cell depletion. *Immunity.* 2001; 15: 801–12.
11. **Umetsu SE, Lee WL, McIntire JJ, *et al.*** TIM-1 induces T cell activation and inhibits the development of peripheral tolerance. *Nat Immunol.* 2005; 6: 447–54.
12. **Huppa JB, Davis MM.** T-cell-antigen recognition and the immunological synapse. *Nat. Rev. Immunol.* 2003; 3: 973–83.
13. **Popescu LM, Gherghiceanu M, Cretoiu D, *et al.*** The connective connection: interstitial cells of Cajal (ICC) and ICC-like cells establish synapses with immunoreactive cells. Electron microscope study in situ. *J Cell Mol Med.* 2005; 9: 714–30.
14. **Lee KH, Dinner AR, Tu C, *et al.*** The immunological synapse balances T cell receptor signaling and degradation. *Science.* 2003; 302: 1218–22.
15. **Fossum S, Mallett S, Barclay AN.** The MRC OX-47 antigen is a member of the immunoglobulin superfamily with an unusual transmembrane sequence. *Eur J Immunol.* 1991; 21: 671–9.
16. **Biswas C, Zhang Y, DeCastro R, *et al.*** The human tumor cell-derived collagenase stimulatory factor (renamed EMMPRIN) is a member of the immunoglobulin superfamily. *Cancer Res.* 1995; 55: 434–9.
17. **Kasinrerk W, Fiebiger E, Stefanova I, *et al.*** Human leukocyte activation antigen M6, a member of the Ig superfamily, is the species homologue of rat OX-47, mouse basigin, and chicken HT7 molecule. *J Immunol.* 1992; 149: 847–54.
18. **Miyauchi T, Masuzawa Y, Muramatsu T.** The basigin group of the immunoglobulin superfamily: complete conservation of a segment in and around transmembrane domains of human and mouse basigin and chicken HT7 antigen. *J Biochem.* 1991; 110: 770–4.
19. **Jiang JL, Zhou Q, Yu MK, *et al.*** The involvement of HAb18G/CD147 in regulation of store-operated calcium entry and metastasis of human hepatoma cells. *J Biol Chem.* 2001; 276: 46870–7.
20. **A randomized controlled trial of Licartin for preventing hepatoma recurrence after liver transplantation.** A randomized controlled trial of Licartin for preventing hepatoma recurrence after liver transplantation. *Hepatology.* 2007; 45: 269–76.
21. **Muramatsu T, Miyauchi T.** Basigin (CD147): a multifunctional transmembrane protein involved in reproduction, neural function, inflammation and tumor invasion. *Histol Histopathol.* 2003; 18: 981–7.
22. **Yan L, Zucker S, Toole BP.** Roles of the multifunctional glycoprotein, emmprin (basigin; CD147), in tumour progression. *Thromb Haemost.* 2005; 93: 199–204.
23. **Gabison EE, Hoang-Xuan T, Mauviel A, *et al.*** EMMPRIN/CD147, an MMP modulator in cancer, development and tissue repair. *Biochimie.* 2005; 87: 361–8.
24. **Nabeshima K, Iwasaki H, Koga K, *et al.*** Emmprin (basigin/CD147): matrix metalloproteinase modulator and multifunctional cell recognition molecule that plays a critical role in cancer progression. *Pathol Int.* 2006; 56: 359–67.
25. **Arora K, Gwinn WM, Bower MA, *et al.*** Extracellular cyclophilins contribute to the regulation of inflammatory responses. *J Immunol.* 2005; 175: 517–22.
26. **Gwinn WM, Damsker JM, Falahati R, *et al.*** Novel approach to inhibit asthma-mediated lung inflammation using anti-CD147 intervention. *J Immunol.* 2006; 177: 4870–9.
27. **Zhu P, Lu N, Shi ZG, *et al.*** CD147 overexpression on synoviocytes in rheumatoid arthritis enhances matrix metalloproteinase production and invasiveness of synoviocytes. *Arthritis Res Ther.* 2006; 8: R44.
28. **Pistol G, Matache C, Calugaru A, *et al.*** Roles of CD147 on T lymphocytes activation and MMP-9 secretion in systemic lupus erythematosus. *J Cell Mol Med.* 2007; 11: 339–48.
29. **Spinale FG, Coker ML, Heung LJ, *et al.*** A matrix metalloproteinase induction/activation system exists in the human left ventricular myocardium and is upregulated in heart failure. *Circulation.* 2000; 102: 1944–9.
30. **Zhou S, Zhou H, Walian PJ, *et al.*** CD147 is a regulatory subunit of the gamma-secretase complex in Alzheimer's disease amyloid beta-peptide production. *Proc Natl Acad Sci USA.* 2005; 102: 7499–504.
31. **Renno T, Wilson A, Dunkel C, *et al.*** A role for CD147 in thymic development. *J Immunol.* 2002; 168: 4946–50.
32. **Koch C, Staffler G, Hüttinger R, *et al.*** T cell activation-associated epitopes of CD147 in regulation of the T cell response, and their definition by antibody affinity and antigen density. *Int Immunol.* 1999; 11: 777–86.
33. **Stonehouse TJ, Woodhead VE, Herridge PS, *et al.*** Molecular characterization of U937-dependent T-cell co-stimulation. *Immunology.* 1999; 96: 35–47.
34. **Allain F, Vanpouille C, Carpentier M, *et al.*** Interaction with glycosaminoglycans is required for cyclophilin B to trigger integrin-mediated adhesion of peripheral blood T lymphocytes to extracellular matrix. *Proc Natl Acad Sci USA.* 2002; 99: 2714–9.
35. **Igakura T, Kadomatsu K, Taguchi O, *et al.*** Roles of basigin, a member of the immunoglobulin superfamily, in behavior as to an irritating odor, lymphocyte response, and blood-brain barrier. *Biochem Biophys Res Commun.* 1996; 224: 33–6.
36. **Gunzer M, Weishaupt C, Planelles L, *et al.*** Two-step negative enrichment of CD4+ and CD8+ T cells from murine

spleen *via* nylon wool adherence and an optimized antibody cocktail. *J Immunol Methods.* 2001; 258: 55–63.

37. **Viola A, Schroeder S, Sakakibara Y, *et al.*** T lymphocyte costimulation mediated by reorganization of membrane microdomains. *Science.* 1999; 283: 680–2.
38. **Viola A.** The amplification of TCR signaling by dynamic membrane microdomains. *Trends Immunol.* 2001; 22: 322–7.
39. **Wang L, Ku XM, Li Y, *et al.*** Regulation of matrix metalloproteinase production and tumor cell invasion by four monoclonal antibodies against different epitopes of HAb18G/CD147 extracellular domain. *Hybridoma.* 2006; 25: 60–7.
40. **Tanser SB, Onfelt B, Pirinen NJ, *et al.*** Control of immune responses by trafficking cell surface proteins, vesicles and lipid rafts to and from the immunological synapse. *Traffic.* 2004; 5: 651–61.
41. **Holt O, Kanno E, Bossi G, *et al.*** Slp1 and Slp2-a localize to the plasma membrane of CTL and contribute to secretion from the immunological synapse. *Traffic.* 2008; 9: 446–57.
42. **Dadsetan S, Zakharova L, Molinski TF, *et al.*** Store-operated Ca^{2+} influx causes Ca^{2+} release from the intracellular Ca^{2+} channels that is required for T cell activation. *J Biol Chem.* 2008; 18: 12512–9
43. **Razzaq TM, Ozegbe P, Jury EC, *et al.*** Regulation of T-cell receptor signalling by membrane microdomains. *Immunology.* 2004; 113: 413–26.
44. **Chentouf M, Ghannam S, Bes C, *et al.*** Recombinant anti-CD4 antibody 13B8.2 blocks membrane-proximal events by excluding the Zap70 molecule and downstream targets SLP-76, PLC gamma 1, and Vav-1 from the CD4-segregated Brij 98 detergent-resistant raft domains. *J Immunol.* 2007; 179: 409–20.
45. **Staffler G, Szekeres A, Schütz GJ, *et al.*** Selective inhibition of T cell activation *via* CD147 through novel modulation of lipid rafts. *J Immunol.* 2003; 171: 1707–14.
46. **Croft M.** Co-stimulatory members of the TNFR family: keys to effective T-cell immunity? *Nat Rev Immunol.* 2003; 3: 609–20.
47. **Smith KA.** Interleukin-2: inception, impact, and implications. *Science.* 1988; 240: 1169–76.
48. **Kuroda K, Yagi J, Imanishi K, *et al.*** Implantation of IL-2-containing osmotic pump prolongs the survival of superantigen-reactive T cells expanded in mice injected with bacterial superantigen. *J Immunol.* 1996; 157: 1422–31.
49. **Paul WE, Seder RA.** Lymphocyte responses and cytokines. *Cell.* 1994; 76: 241–51.
50. **Yamazaki T, Akiba H, Koyanagi A, *et al.*** Blockade of B7-H1 on macrophages suppresses CD4+ T cell proliferation by augmenting IFN-gamma-induced nitric oxide production. *J Immunol.* 2005; 175: 1586–92.
51. **Wu X, Hou W, Sun S, *et al.*** Novel function of IFN-gamma: negative regulation of dendritic cell migration and T cell priming. *J Immunol.* 2006; 177: 934–43.
52. **Yu XL, Hu T, Du JM, *et al.*** Crystal structure of HAb18G/CD147: implications for immunoglobulin superfamily homophilic adhesion. *J Biol Chem.* 2008; 283: 18056–65.
53. **Ku XM, Liao CG, Li Y, *et al.*** Epitope mapping of series of monoclonal antibodies against the hepatocellular carcinoma-associated antigen HAb18G/CD147. *Scand J Immunol.* 2007; 65: 435–43.
54. **Yoshida S, Shibata M, Yamamoto S, *et al.*** Homo-oligomer formation by basigin, an immunoglobulin superfamily member, *via* its N-terminal immunoglobulin domain. *Eur J Biochem.* 2000; 267: 4372–80.